



ELSEVIER

Journal of Chromatography A, 832 (1999) 211–224

JOURNAL OF  
CHROMATOGRAPHY A

# Selective fluorescence derivatization and capillary electrophoretic separation of amidated amino acids

Lei Feng, Mitchell E. Johnson\*

*Duquesne University, Department of Chemistry and Biochemistry, 308 Mellon Hall of Sciences, Pittsburgh, PA 15282-1530, USA*

Received 25 August 1998; received in revised form 17 November 1998; accepted 17 November 1998

## Abstract

Selectively derivatized amide-terminated amino acids were separated by micellar electrokinetic capillary chromatography (MECC). The amides were selectively derivatized by deactivating all primary amines in the sample mixture by acetylation, converting the amides to primary amines by Hofmann rearrangement, and tagging the resultant amines with fluorescein isothiocyanate (FITC). The fluorescent amide derivatives were detected by confocal laser-induced fluorescence. The use of the MECC mode was mandated by very similar charge and size characteristics of the derivatized amides. Separation of 11 amino acid amides was carried out in bare fused silica capillaries in 10 mM borate and 90 mM sodium dodecyl sulfate buffer in under 15 min. Analysis of dispersion and mobility behavior suggests that hydrophobicity is the primary determinant of micelle/buffer partitioning, and, therefore, mobility; relative hydrophobicity based on values for amino acids is an adequate predictor of elution order for derivatives without charged side-chains. Selectivity of the reaction was estimated to be as great as 100, perhaps greater; the estimation was limited by ability of FITC to derivatize at low concentrations. Rearrangement reaction yields and kinetics were found by NMR spectroscopy to depend on side-chain identity. Yields were 80–100% for the rearrangement, and half-lives were 10–30 min for 100 mM solutions of several representative amino acid amides. Reaction products were not purified, for the sake of simplicity, and a number of impurity peaks appeared in the electropherograms. Because of the high efficiency of the separation (optimal plate heights below 2  $\mu\text{m}$ ), resolution was usually adequate to mitigate this potential problem. © 1999 Elsevier Science B.V. All rights reserved.

**Keywords:** Derivatization, electrophoresis; Amino acids; Acetylamino acid amides; Peptides; Hormones

## 1. Introduction

Amidation at the carboxy terminus is essential to biological activity in at least half of known peptide hormones [1]. Amidation is the ultimate step in post-translational processing of peptide hormones, wherein the enzyme peptidylglycine  $\alpha$ -amidating monooxygenase cleaves a glycine from the prohor-

mone, leaving the amide instead of the carboxylic acid [2]. Disruption of this processing step often accompanies tumor production [3–9] and is implicated in several other diseases [10–12]. Because hormone production is highly regulated, and because hormones are very potent in their effects, the importance of the development of ultrasensitive methods for the detection of peptide hormones is manifest.

Tatemoto and Mutt pioneered a chemical method for amidated peptide hormone detection [13]. This method relies on sample prefractionation (traditional-

\*Corresponding author. Tel.: +412-396-5278; fax: +412-396-5683; e-mail: johnsonm@duq.edu

ly, extensive column chromatography which has since been replaced by solid-phase extraction and HPLC [14]), enzymatic digestion of the peptides, derivatization of the resulting amino acids and peptide fragments with dansyl chloride, and selective extraction of the dansylated amino acid amides from high-pH aqueous buffer with ethyl acetate. Phenyl isothiocyanate has also been used instead of dansyl chloride [14]. The amides are subsequently identified by thin-layer chromatography [13] or by HPLC [14,15]. The selectivity of these methods relies entirely on the selectivity of the extraction of the less polar, uncharged, derivatized amino acid amides into ethyl acetate. The degree of extraction depends on the identity of the amide and the derivatization reagent, and is greater than 90% for most amides [14,15]. Although this overall scheme provides little information on peptide structure, it is very useful for screening HPLC column fractions for peptide amides. However, selectivity of the detection step, depending as it does on extraction, is not particularly high.

Hill et al. employ a slightly different scheme [16]. The amine functionalities on the peptides in each column fraction are acetylated, the amides are converted to primary amines via Hofmann rearrangement, and the resultant amines (which derive solely from primary amides) are tagged with ninhydrin for colorimetric detection. Fractions are also screened for glycine-terminal peptides (i.e., prohormones) with a single carboxy-terminus Edman-type reaction and HPLC detection. Coincidence of amide and glycine terminus is a strong indicator of hormone presence.

The strength of the Hill, Flannery, and Fraser scheme lies in its selectivity, which is based on the ability to deactivate primary amines prior to derivatization. Selectivity is potentially much higher than for simple extraction. We have chosen to combine the strengths of the two approaches: fractionation and digestion, followed by acetylation of the amino acid and amino acid amide amine functionalities, conversion of the amides to amines, derivatization of the amines with a high-efficiency fluorophore, and detection by capillary electrophoresis with confocal laser-induced fluorescence detection (CE-LIF). The use of CE-LIF was motivated primarily by the need for high mass and

concentration sensitivity; LIF has the highest reported sensitivity as a detection mode for separations [17]. We report here separation and detection conditions for several *N*-acetylamino acid amide fluorescein isothiocyanate derivatives and preliminary estimates of the selectivity of this scheme. To the best of our knowledge, this is the first report of derivatization of the amide functionality for detection in capillary electrophoresis. Amides derivatized at the amine terminus have been separated by HPLC [14,15] and CE [18]; the latter work showed that amide and carboxy terminal amino acids exhibit very different electrophoretic behavior. The amide functionality is not particularly reactive, but it can be derivatized directly by silylation for GC-MS analysis [19].

## 2. Experimental

### 2.1. Electrophoresis

Capillaries were unmodified fused silica of 25  $\mu\text{m}$  I.D.  $\times$  363  $\mu\text{m}$  O.D. (Polymicro Technologies, Phoenix, AZ, USA). A section ( $\sim$ 10 mm) of the polyimide coating was gently burned off with a butane torch to provide a detection window, and the capillary was mounted on a glass microscope slide with epoxy. Polyethylene or glass vials of 0.5–2.0 ml were used as reservoirs for buffer, sample, and waste solutions. The inlet and outlet of the capillary were enclosed in Lexan boxes equipped with safety switches. Platinum electrodes were inserted from the top of the safety boxes into the vials. A syringe pump (Harvard Apparatus 975, South Natick, MA, USA) driven polyethylene syringe was used for capillary filling, equilibration, and flushing. Voltage was supplied by a 30 kV high-voltage power supply (Spellman 1000R CZE, Plainview, NY, USA). The inlet was grounded, and negative voltage was applied to the outlet. All samples were injected electrokinetically at 5–20 kV for 1–10 s. Voltage was adjusted manually on the power supply, and injection time was controlled either manually with the aid of a stopwatch or with a custom-made electronic timer.

Borate electrophoresis buffer was prepared by dissolving the appropriate amount of sodium tetraborate decahydrate in distilled, deionized water

(DDI, Barnstead Nanopure, Barnstead/Thermolyne, Dubuque, IA, USA 17.8–18 M $\Omega$ cm) and adjusting the pH with high purity HCl or NaOH, as required. Samples were dissolved in the electrophoresis buffer. The formal borate concentration was 10 mM in all cases. Running buffer for micellar electrokinetic capillary chromatography (MECC) was prepared by adding the appropriate amount of sodium dodecylsulfate (SDS) directly to the borate buffer. All buffers were filtered with a 0.2  $\mu$ m nylon membrane filter prior to use.

### 2.2. Confocal laser-induced fluorescence detection

The confocal LIF detector has been described in detail elsewhere [20]. Excitation was provided by an air-cooled argon-ion laser (American Laser LS1000, Salt Lake City, UT, USA) operating at 488.0 nm. The collimated laser beam was reflected by a dichroic beamsplitter (505DRLP, Omega Optical, Brattleboro, VT, USA) into a 40 $\times$ , 0.85 NA microscope objective (Fluor 40, Nikon, Tokyo, Japan). The objective focused the laser light into the electrophoresis capillary and collected the fluorescence. The fluorescence was passed by the beamsplitter and was focused onto a 600  $\mu$ m (for the 25  $\mu$ m I.D. capillary) or 800  $\mu$ m (50  $\mu$ m I.D. capillary) pinhole (National Aperture, Salem, NH, USA or Melles Griot, Irvine, CA, USA). Light was filtered by an interference bandpass filter at 525 nm $\pm$ 20 nm (Omega Optical). The remaining fluorescence was collected and focused by a pair of achromats (12.5 mm dia., 24 mm effective focal length, Rolyn Optics, Covina, CA, USA) onto the active area of an actively-quenched, photon counting, avalanche photodiode (SPCM-AQ-141, EG and G Optoelectronics Canada, Vaudreuil, Canada). The SPCM module also amplified and discriminated the photoelectron pulses, and the TTL output was sent to a multichannel scaler card (MCS-II, Oxford Tennelec/Nucleus, Oak Ridge, TN, USA) residing in a 486 PC-compatible computer.

### 2.3. Amide derivatization

Fresh 0.12–0.15 M phenyliodolyl bis(trifluoroacetate) [PIFA, or phenylbis(trifluoroacetato-O)-iodine] was prepared by dissolving PIFA in DDI water–

acetonitrile (1:1, v/v). Twenty  $\mu$ mol of *N*-acetylamino acid amide (AAAA) was weighed into a glass vial and 200  $\mu$ l of PIFA reagent solution was added for every 20  $\mu$ mol AAAA. Ultrasonication for 1–3 min helped to dissolve the AAAA and also ensured good mixing. The reaction mixture was kept in the dark overnight. Then 5  $\mu$ l of the PIFA reaction mixture was mixed with 95  $\mu$ l of 0.1 mM fluorescein isothiocyanate (FITC) in 10 mM borate buffer (pH 9). The derivatization mixtures were again placed in the dark to react overnight. The derivatization mixtures were diluted with 10 mM borate buffer to obtain 1–100 nM injection samples.

NMR was used to follow the kinetics of the amide-to-amine conversion. Three solvents,  $^2\text{H}_2\text{O}$ , [ $^2\text{H}_4$ ]methanol, and [ $^2\text{H}_6$ ]acetone, served as the reaction solvent, either alone or in combination, depending on the solubility of the AAAA. For each reaction, 0.1 mmol of AAAA and 0.15 mmol of PIFA were dissolved separately in 500  $\mu$ l of deuterated solvent and filtered with a glass wool filter. The two solutions were quickly mixed in an NMR tube and lowered immediately into the sample chamber of a 300 MHz NMR (Bruker AC300, Karlsruhe, Germany). Spectra were collected at regularly timed intervals.

### 2.4. Acetylation protection of the amino group

Samples were weighed into 2 ml glass vials. At least 100  $\mu$ l of acetic anhydride and pyridine each were then added for every 20  $\mu$ mol of sample. The reactions were kept at 60 $^\circ$ C for 1 h. The reaction mixture was then cooled to 40 $^\circ$ C and the unreacted reagents were removed by bubbling dry nitrogen through the solution. The acetylation products were then subjected to the PIFA amide-to-amine conversion and FITC derivatization procedures described above.

### 2.5. Materials and reagents

Amidated amino acids and *N*-acetyl amidated amino acids were obtained from BAChem (King of Prussia, PA, USA). Deuterated NMR solvents  $^2\text{H}_2\text{O}$ , [ $^2\text{H}_4$ ]methanol, [ $^2\text{H}_6$ ]acetone, PIFA, and SDS were obtained from Sigma (St. Louis, MO, USA). Sodium

tetraborate decahydrate was purchased from Fisher (Pittsburgh, PA, USA). All reagents were used as received, without further purification.

### 3. Results and discussion

#### 3.1. Amide-to-amine conversion

Louden and coworkers have developed the means to convert primary amides to primary amines via a Hofmann rearrangement (Fig. 1) [21–23]. The reaction is carried out under acidic conditions in aqueous–acetonitrile solution at room temperature with generally greater than 70% yield. The original procedure, adapted from that of Hill et al. [16], included termination of the PIFA reaction with HCl and extraction of unreacted PIFA and its corresponding reaction product from the reaction mixture with toluene. It was then necessary to add concentrated NaOH solution to the aqueous phase to adjust the pH to basic before it could be used in the FITC derivatization reaction. However, simple dilution of the PIFA reaction mixture in pH 9 FITC reaction buffer was found to yield essentially identical results. Loudon et al. have also shown that the use of

pyridine as a catalyst will increase reaction rates 30–50 fold; however, pyridine was not used extensively because it introduced interferences in the NMR spectra and in electropherograms. Saby et al. have reported somewhat different reaction conditions in the use of PIFA as an oxidizing reagent for chlorophenols [24].

In order to examine the efficiency of this reaction, the PIFA reaction was followed by NMR. The signals corresponding to the protons attached to carbons marked with an asterisk in Fig. 1 were monitored during the course of the reaction, as were protons on the side chains in some cases. Quantitation was achieved by simple peak integration. Results were consistent regardless of the proton signal monitored. The results for four AAAA's are shown in Fig. 2. Reaction yields were quite good, with quantitative yields for *N*-acetylvalinamide and *N*-acetylphenylalaninamide in less than 2 h. Yield was worst for *N*-acetylleucinamide, but it was still greater than 70% complete within an hour. *N*-acetylalaninamide was the slowest reactant, but it reached 80% yield in 3 h. These results were comparable to those reported by Loudon et al., who found yields of 79% and 75% for *N*-acetylphenylalaninamide and *N*-acetylvalinamide, re-

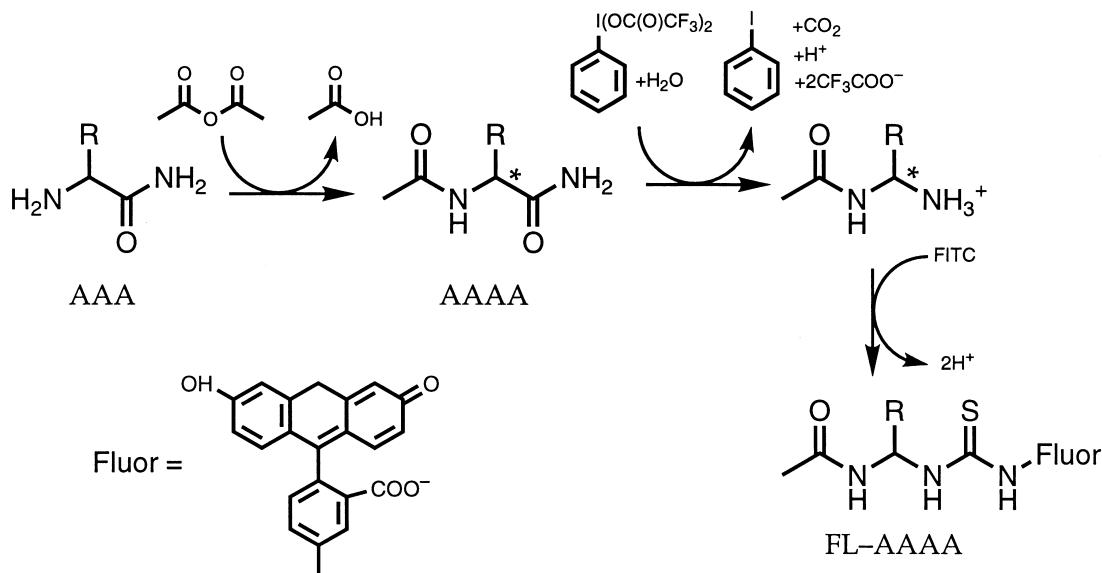


Fig. 1. Selective derivatization scheme for amino acid amides and related amides. R is the amino acid amide side chain. Asterisk indicates proton followed by NMR for kinetic studies. Fluor=fluoresceinyl; the thiocarbonyl linkage is shown explicitly.

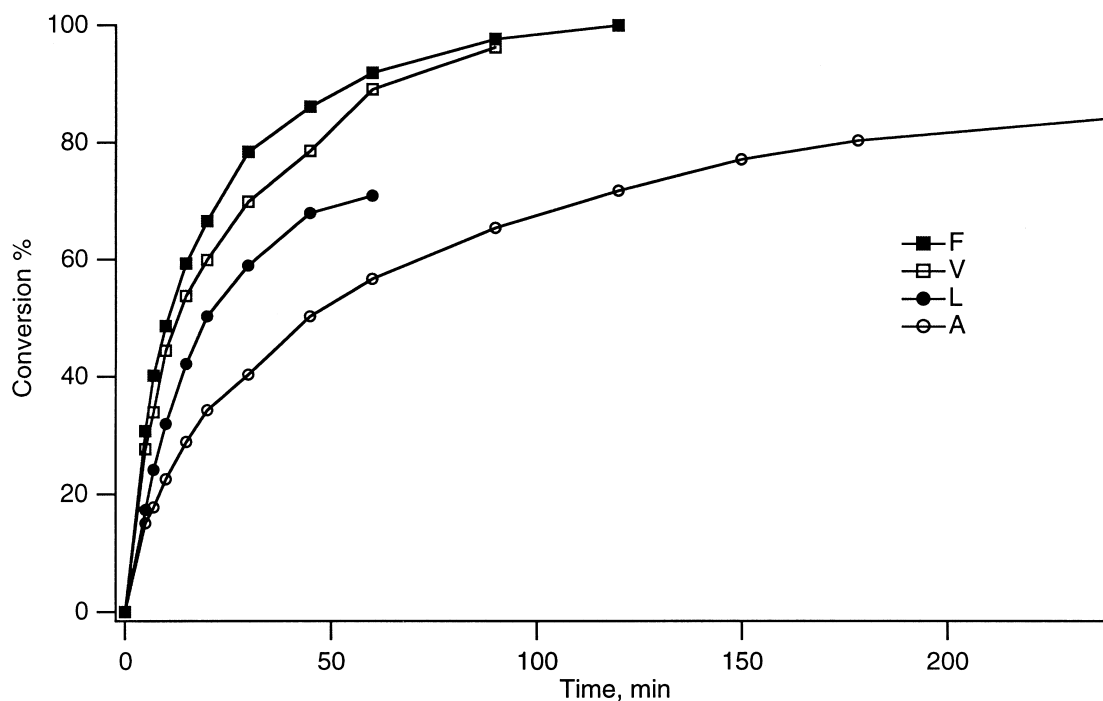


Fig. 2. PIFA conversion of *N*-acetylamino acid amides to corresponding primary amines as a function of time. Each point corresponds to % conversion as determined by comparison of peak heights on the NMR spectrum of the reaction mixture. Monitored proton peaks are marked with asterisks in Fig. 1. Species are identified according to their corresponding one-letter amino acid abbreviation throughout. Solid lines are provided for visual purposes and are not a fit to the data (see text).

spectively [23]. The actual rate law derived by Boutin and Loudon is moderately complex [22]. The reaction depends strongly on pH and the formation of a PIFA dimer. Thus, the simple NMR experiment did not yield enough data to extract rate constants. However, the rates observed were comparable in magnitude with those observed by Boutin and Loudon under similar conditions. These reaction conditions are acceptable for off-column derivatization, as they are comparable in yield and reaction time to most fluorescent isothiocyanates and succinimidyl esters. The overnight reaction times employed in subsequent work ensured completion of all reactions, though not necessarily 100% yield, and the products were stable as long as they were used for further reaction within a day.

### 3.2. Capillary electrophoretic separation

Capillary electrophoresis in the free zone mode (FZE) is a very simple, fast, and efficient mode for

those analytes that have different charge-to-size ratios. It has been widely used to separate amino acids and their derivatives [25]. Because of the zwitterionic character of amino acids, buffer pH is the most important parameter affecting separation order and efficiency. However, fluorescein quantum efficiency is optimum in the pH range 8–10; a borate buffer at pH 9 was used to separate all fluorescein derivatives in this work. Organic modifiers such as methanol and acetonitrile were useful in separating amino acids in the free zone mode; 9 of 11 FITC-derivatized amino acids corresponding to the amides used in this work were separated in a 10 mM borate buffer containing 10% acetonitrile (data not shown).

Although derived from amino acids, the *N*-acetylamino acid amide derivatives (FL-AAAs, see Fig. 1) behaved quite differently in electrophoresis. The modification of their amino ends through acetylation and their original carboxyl ends through amide–amine conversion and attachment of the FITC tag eliminated the possibility of charge variation in

these parts of the molecules (fluorescein has approximately unit negative charge at pH 9). Differentiation of this series of analytes was focused on the side chain differences, and, therefore, on hydrophobicity differences. The FZE mode was no longer sufficient for this purpose, and the MECC mode was required to achieve good separation.

In the MECC mode, the effective mobility of the analyte is a weighted average of the intrinsic mobilities of the analyte and micelle, with the weighting factors being the mole fraction in either buffer or micelle [25]. For a given electrophoresis condition, the net analyte mobility is determined by its electrophoretic mobility and its degree of partitioning of the analyte between the buffer and micelles (NB “electrophoretic mobility” in this case refers to the intrinsic, free zone mobility in the absence of micelles and electroosmotic flow). For amino acid amides that have been derivatized as described above, there is no charge variation among the compounds except for cases in which the side-chain is either ionized (e.g. tyrosine) or derivatized (e.g. glutamine). The separation is, therefore, effected primarily by differential partitioning of the analytes in the micelles and secondarily by minor differences in mobility due to differences in size and shape. The relative retention is therefore expected to correlate primarily with the hydrophobicity of the amino acid amide side chain.

Fig. 3a shows the separation of 11 amino acid amide derivatives. For convenience, the derivatives are referred to by the one-letter designation of their corresponding amino acids. In this case, commercial *N*-acetyl amino acid amides were reacted with PIFA and FITC separately and mixed and diluted prior to injection. Identity of the peaks was established by multiple spiking experiments and by individual mobilities.

For those compounds whose side-chains are not ionized or otherwise derivatized, elution order is largely predictable on the basis of side-chain hydrophobicity. Elution order is best predicted for M (−5.92), W (−5.84), V (−13.02), I (−16.71), and L (−16.71) (values in parentheses are hydrophobicity values derived from partitioning coefficients for side-chain analogs in water: cyclohexane, in kJ/mol [26]). Alaninamide (−3.65 kJ/mol) and phenylalanine (−8.57 kJ/mol) derivatives eluted later than

expected. The above treatment, of course, neglects differences in electrophoretic mobility, which, though too small for separation, were not negligible. Isoleucinamide and leucinamide derivatives have different elution times despite identical hydrophobicity due to shape selectivity in electrophoresis, or, perhaps, in partitioning. Alaninamide probably has a higher electrophoretic mobility, and, therefore, lower net mobility (intrinsic mobility is towards the injector). However, there is some evidence that phenylalanine partitions more strongly into the micelles than is predicted by this hydrophobicity model system. *N*-octanol–water partitioning data for *N*-acetyl phenylalaninamide shows a value much closer to isoleucinamide and leucinamide (−7.49 vs. −7.53 and −7.12 kJ/mol, respectively [26]). Bennett and Solomon showed that *N*-phenylisothiocyanate-derivatized phenylalaninamide eluted almost last among other amides from a C<sub>18</sub> RP-HPLC separation [14]. Also, dispersion data (see below) show that phenylalaninamide is strongly partitioned into the micelles.

The remaining derivatives have modified side-chains. Tyrosinamide (4.54 kJ/mol) is relatively hydrophilic, and should have eluted before methioninamide, but had a partial negative charge on its side-chain at pH 9 ( $pK_a=10.07$ ). There was probably a tradeoff between micelle repulsion (less partitioning) and increased electrophoretic mobility towards the injector (lower net mobility). The derivative structures of glutaminamide and lysinamide should have been fairly similar: the amide side-chain of glutaminamide was oxidized with PIFA and derivatized with FITC, and the lysinamide side-chain was also derivatized with FITC. The lysinamide in this case was commercially *N*-acetylated, and the side-chain retained the free amine. Thus, both had an extra negative charge in addition to the extra fluoresceinyl group, and electrophoretic mobility and partitioning were both affected. In no case did we observe multiple derivatives. Charge repulsion from the micelle apparently operated most strongly with the glutaminamide derivative, and it eluted very early, whereas the longer side-chain of lysinamide apparently allowed stronger partitioning, and it eluted last.

While these simple models and arguments are not perfect, they seem to provide enough of an under-

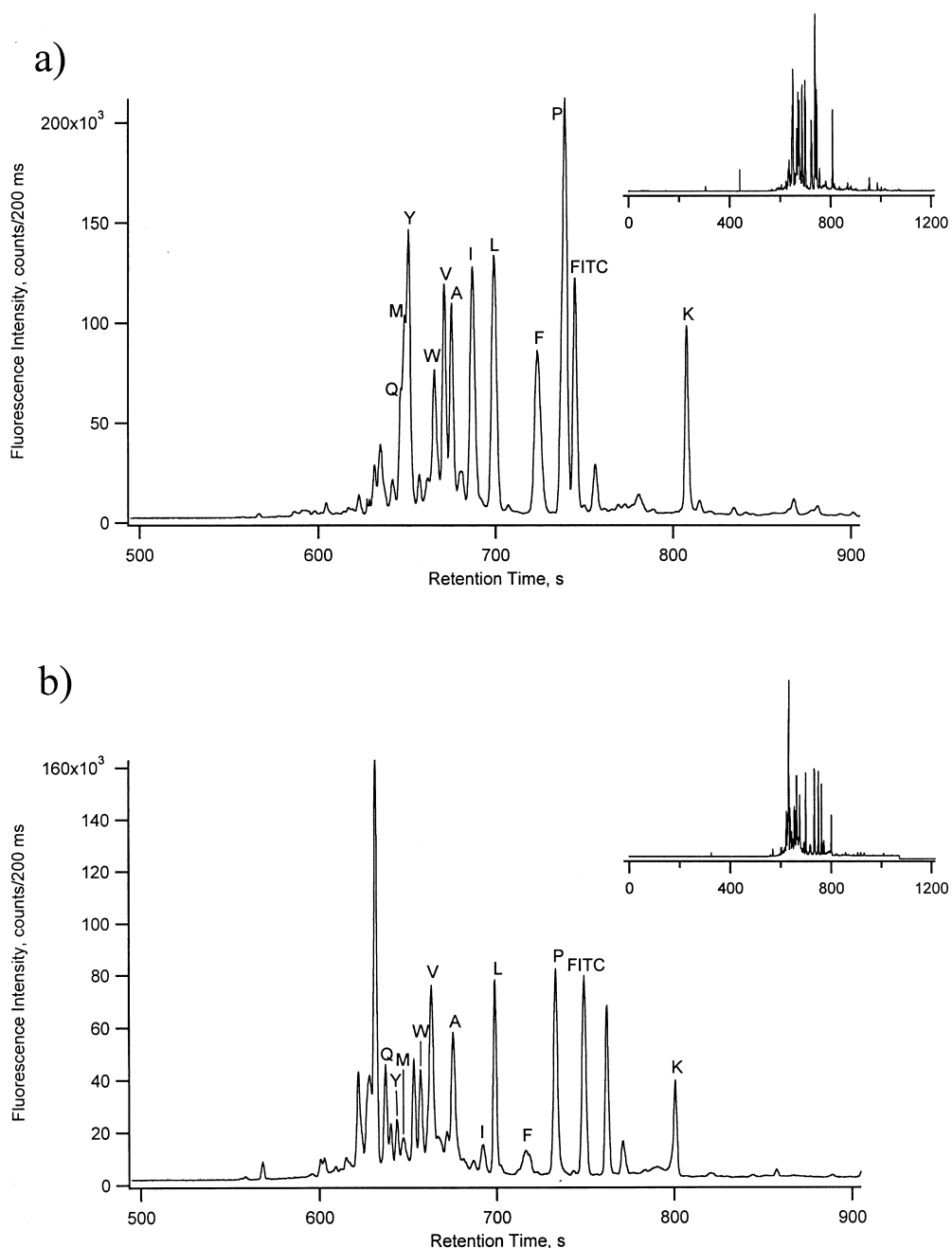


Fig. 3. MECC separation of FITC derivatives of 11 oxidized *N*-acetylamino acid amides (i.e., FL-AAAAs, see Fig. 1). Sample prepared by: (a) mixing individually PIFA- and FITC-derivatized *N*-acetyl amino acid amides (PIFA conversion at 100 mM, FITC derivatization at 5 mM, injection at 70 nM each except Q, W at 350 nM and Y at 140 nM, assuming 70% FITC derivatization efficiency), and (b) mixing *N*-acetyl amino acid amides then derivatizing with PIFA and FITC (PIFA conversion at 9 mM each, FITC derivatization at 5 mM each, injection at 50 nM each). Capillary: 80 cm (effective length 57.5 cm)  $\times$  25  $\mu$ m I.D.,  $\times$  363  $\mu$ m O.D. Buffer: 10 mM borate, 90 mM SDS, pH 9.2. Injection at 20 kV for 3 s, manual, and electrophoresis at 20 kV, 3.7  $\mu$ A.

standing of the separation behavior of these compounds to further improve separations. Resolution was only problematic for those compounds that did not partition strongly into the micelles, which suggests a need for mixed micelles or micellar gradient elution.

Fig. 3a and b compare the results of derivatizing individual *N*-acetylamino acid amides to derivatizing a mixture of amides. The two separations were quite similar, but a number of additional interfering peaks (unidentified) appeared in the latter separation. While the stoichiometry was maintained for the mixture (Fig. 3b), the concentration at derivatization was lower by a factor of 11 for individual amide derivatives than when derivatized individually. Therefore, the additional peaks observed in Fig. 3b may have resulted from the different reaction conditions; it is not uncommon to observe additional interfering peaks as the derivatization concentration is lowered [27,28]. However, the efficiency of the latter separation was somewhat better, and the first three peaks were better resolved. Resolution could be improved by perhaps as much as 50% by reducing the surfactant concentration (see below), but was quite sufficient for separation of most test compounds from each other and from most of the interfering peaks.

Aside from differences caused by concentration differences between the two injections, other slight differences in relative peak heights can be attributed to relative differences in PIFA and FITC reaction efficiency and fluorescence quantum yield. The FITC derivatization required a large excess of either amine or FITC; a 50-fold excess of amine, for example, typically gave a reaction efficiency of only 70%. Differences in the rates of reaction for both PIFA and FITC reactions will also affect peak height in cases where a mixture is derivatized in the presence of a limiting amount of reagent, as is the case in Fig. 3b. *N*-acetylisoleucinamide and phenylalaninamide were most affected. *N*-acetylphenylalaninamide had the fastest oxidation rate (Fig. 2); however, its low yield could have been due to poor FITC derivatization efficiency at the lower concentration. Without independent data on FITC kinetics and fluorescence quantum yield, it is impossible to determine quantitatively the relative contribution of these effects.

Peak dispersion, given in terms of theoretical plate height, as a function of applied voltage gives signifi-

cant information on the electrophoretic behavior. Plate height data are shown in Fig. 4 for several amino acid amide derivatives and FITC in 50 mM SDS. At high field strength and optimum SDS concentration (~50 mM, see below), plate height was quite good. Nearly  $10^6$  plates/m were achieved in these separations. In addition, the dispersion characteristics of a compound give some indication of its degree of association with the SDS micelles. Molecules that interact with the micelles have an effective diffusion coefficient that is a weighted average of the associated and dissociated molecules (as with mobility, see above). Thus, molecules that interact strongly with micelles have much smaller effective diffusion coefficients, and will show less variation in dispersion with electric field than those molecules that interact very little with the micelles, at least in the absence of mass-transport induced dispersion. It can be seen that FITC dispersion was a strong function of electric field. Therefore, it is reasonable to assume that FITC was retained little, if at all, by the micelles. However, dispersion was not completely due to diffusion only. The plate height for FITC was not strictly hyperbolically related to electric field strength; therefore, additional sources of dispersion were present, such as Joule heating or resistance to mass transport, which prevented any sort of quantitative assignment of partitioning parameters. Ohm's law (current–voltage) plots showed a very slight curvature throughout the applied voltage range, indicating a small amount of Joule heating. However, the qualitative behavior was consistent with overall retention order. The diffusion behavior of the phenylalaninamide derivative, which was strongly retained (Fig. 3), was not affected at all by applied voltage, while leucinamide and alaninamide derivatives were increasingly affected. This confirms the assertion that phenylalaninamide eluted later because of stronger partitioning than predicted by hydrophobicity models. On the other hand, alaninamide behaved in a manner more consistent with a less hydrophobic molecule, which was consistent with the hydrophobicity data, and which suggests that the reason for later elution was indeed due to electrophoretic factors.

The effect of increasing concentration of surfactant on the separation of a number of hydrophobic FL-AAAs is shown in Fig. 5. Retention time



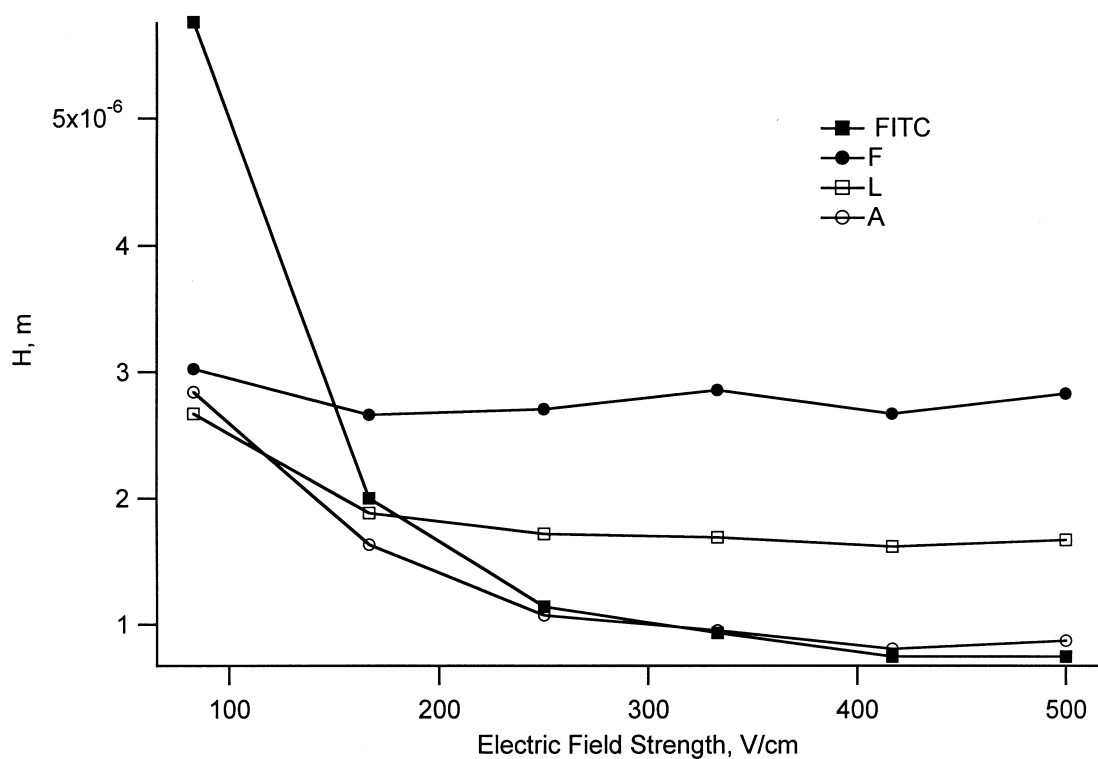


Fig. 4. Theoretical plate height as a function of applied separation voltage for several derivatives and FITC. Capillary: 60 cm (effective length 38 cm) × 25  $\mu\text{m}$  I.D., × 363  $\mu\text{m}$  O.D. Buffer: 10 mM borate, 50 mM SDS, pH 9.2. Injection at 15 kV for 3 s, electronically timed. 35 nM injected for each derivative.

increased for all solutes, including FITC (Fig. 5a–d), as a function of SDS concentration. Two effects change mobility upon increasing surfactant load: differences in electroosmotic mobility due to viscosity and ionic strength increase, and a change in the degree of partitioning into the micelles as the phase ratio is increased. At higher currents, where significant Joule heating occurs, the higher temperature will also change the partition coefficient and decrease viscosity, offsetting the other effects to some extent (or completely [29]). In principle, only viscosity changes should affect intrinsic electrophoretic mobility of both analyte and micelle as surfactant concentration changes, as long as the surfactant concentration is well enough above the critical micelle concentration (CMC, ca. 8 mM for SDS) to ensure relatively monodisperse micelles and is low enough to ensure independent micelles. That is, increasing micelle concentration increases the num-

ber of micelles, but not their size. As discussed above, FITC did not partition strongly into the micelles; therefore its increased retention time was due mainly to a decrease in electroosmotic mobility. Note that the electroosmotic mobility change was reduced in going from 50 to 75 mM, probably due to the compensatory effects of temperature rise.

Therefore, if electroosmotic mobility changes are accounted for with FITC, only the changing phase ratio should determine the relative changes in net mobility of the derivatized AAAAs. Viscosity changes probably do not affect relative mobility significantly because the hydrodynamic radii of the derivatives, as shown by free zone data, are not different enough to show a large dependence on viscosity. In order to calculate retention factors ( $k'$ ), values for dead time (from electroosmotic flow) and micelle elution time are required [29]. However, no micelle or void tracers were used in this work. An

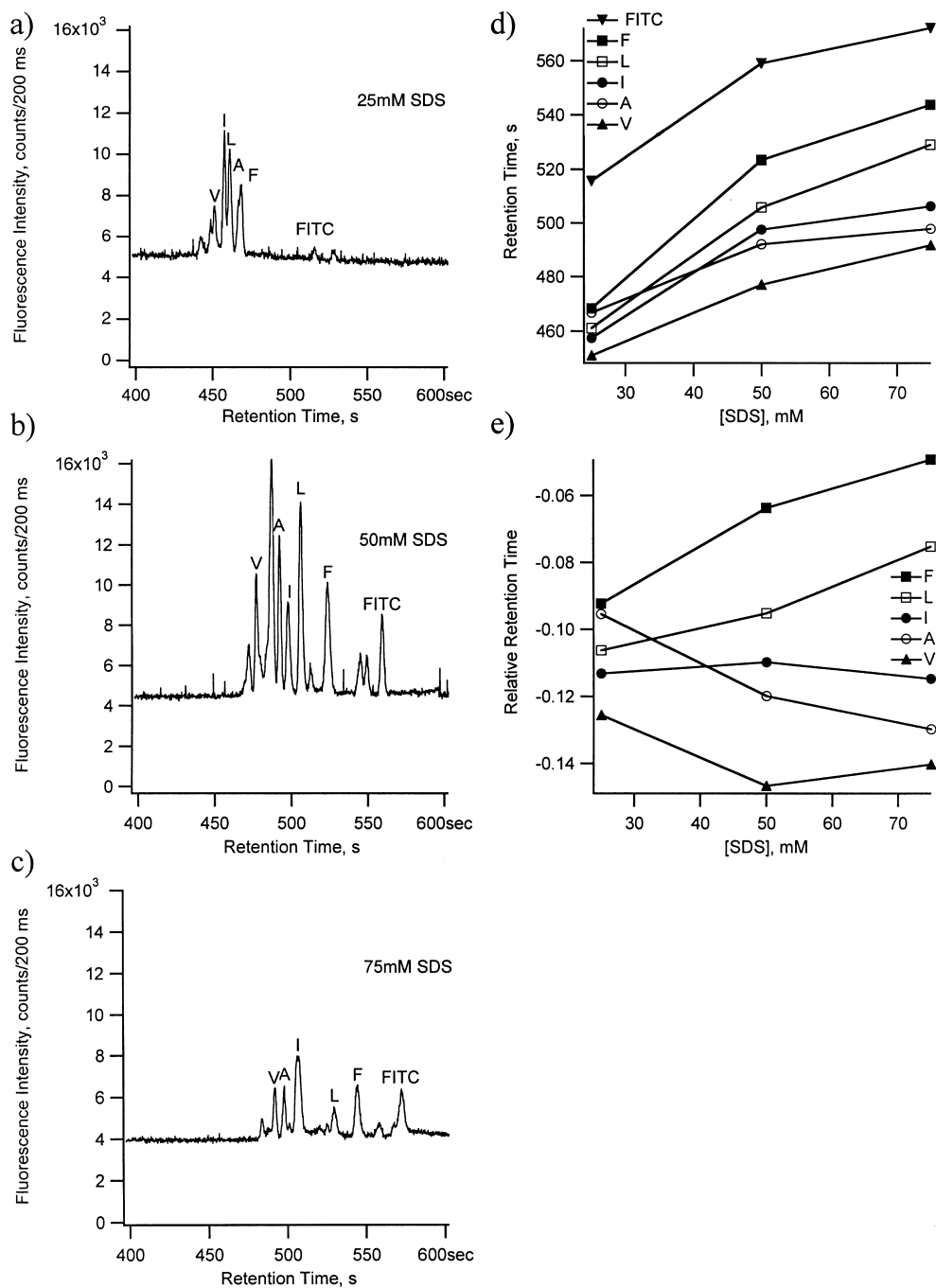


Fig. 5. (a–c) MECC separation of FL-AAAA derivatives in 10 mM borate + (a) 25 mM SDS (b) 50 mM SDS, (c) 75 mM SDS; (d) absolute retention times; (e) relative retention times. Electrophoresis at 20 kV; other conditions as in Fig. 4. Injected concentrations: A 7 nM, V 11.2 nM, L, I, F 1.4 nM each.

effective relative retention time ( $k''$ ) that is exactly analogous to the capacity factor used in liquid chromatography can be calculated as

$$k'' = \frac{t_r - t_{\text{FITC}}}{t_{\text{FITC}}}$$

where  $t_r$  is the observed retention time and  $t_{\text{FITC}}$  is the retention time for free FITC. Fig. 5e shows the calculated relative retention times. The behavior of the derivatives was roughly consistent with hydrophobicity, with the phenylalaninamide derivative showing the strongest retention increase, followed by leucinamide, isoleucinamide, valinamide, and alaninamide derivatives. The alaninamide derivative relative retention time actually decreased, suggesting a distribution coefficient that favored the mobile phase. Thus, alaninamide behaved as expected from hydrophobicity data (i.e., least hydrophobic) but not from the observed separation data, leading again to the suggestion that the discrepancy noted above in the elution order is due to electrophoretic factors; perhaps the size difference between alaninamide and the other hydrophobic amide derivatives was significant enough to decrease its net mobility enough to change its position in the elution order. Note that this treatment retains the correct information regarding observed elution order.

Because of the increased retention time, efficiency also decreased with increasing surfactant concentration. The effect was generally stronger for unretained solutes, though overlap of peaks prevents reliable estimates of plate height, especially at 25 mM SDS. The efficiency of the separation shown in Fig. 3 is probably not optimal at 90 mM SDS, but the larger number of peaks also requires greater retention for resolution, especially for the polar eluents. The relative and absolute peak heights also change considerably with SDS concentration, but the reasons for this are unknown. Quantitative estimates of fluorescence quantum yield are required.

### 3.3. Selective derivatization of amino acid amides

In terms of the selectivity of the fluorescence derivatization reaction, the efficiency of the acetylation step effectively determines the maximum toler-

ance for interferences. There are numerous primary amines available for derivatization in biological fluid extracts and tissue homogenates [30]. Therefore, in order to provide assurance that a detected peak corresponds to an amide, and to minimize interfering peaks in MECC, the derivatization procedure (Fig. 1) must provide a high degree of deactivation of the interfering primary amines. This includes the amino termini of the amino acid amides, as this site would provide two derivatization sites, thus introducing the possibility for multiple peaks for a single amide. Fig. 6 shows a demonstration of derivatization selectivity. The top traces show FITC derivatives of alanine and alaninamide (i.e., the amino terminus was derivatized). Note that these two compounds were easily separated at pH 9. The electropherograms resulting from derivatization of alaninamide per Fig. 1 are shown in the next three traces. The peak for the derivative was easily identified and was well-separated from the other (fairly similar) compounds. There were no peaks corresponding to the homologous amines, even though, in all cases, the initial concentration of alanine in the reaction solution was 33 mM. The smaller peaks in the lower three traces are due to reaction byproducts; the differences in retention times for the peaks at 185 s and the alanine and alaninamide peaks were too great to be explained by retention time irreproducibility. The derivatization of alaninamide failed at 0.1 mM, probably because of poor derivatization properties of FITC. The efficiency of the FITC reaction depended very strongly on relative concentrations of reactants (see above). That being the case, 1% un-acetylated alanine would not be derivatized and detected either. Thus, the selectivity was greater than ten, and was probably much higher. More reactive dyes are being tested that will allow a better estimate of the absolute selectivity.

A demonstration of the analysis of a mixture of amino acid amides using the selective fluorescence derivatization scheme is given in Fig. 7. The scheme worked readily on the mixture, though there was some loss of sample in the mixture (Fig. 7b) for unknown reasons. No extraneous peaks were introduced. Changes in relative peak height between Fig. 7a and b probably reflected differences in reaction kinetics, as discussed above. The data shown in Fig. 7 were more suggestive of the relative PIFA kinetics

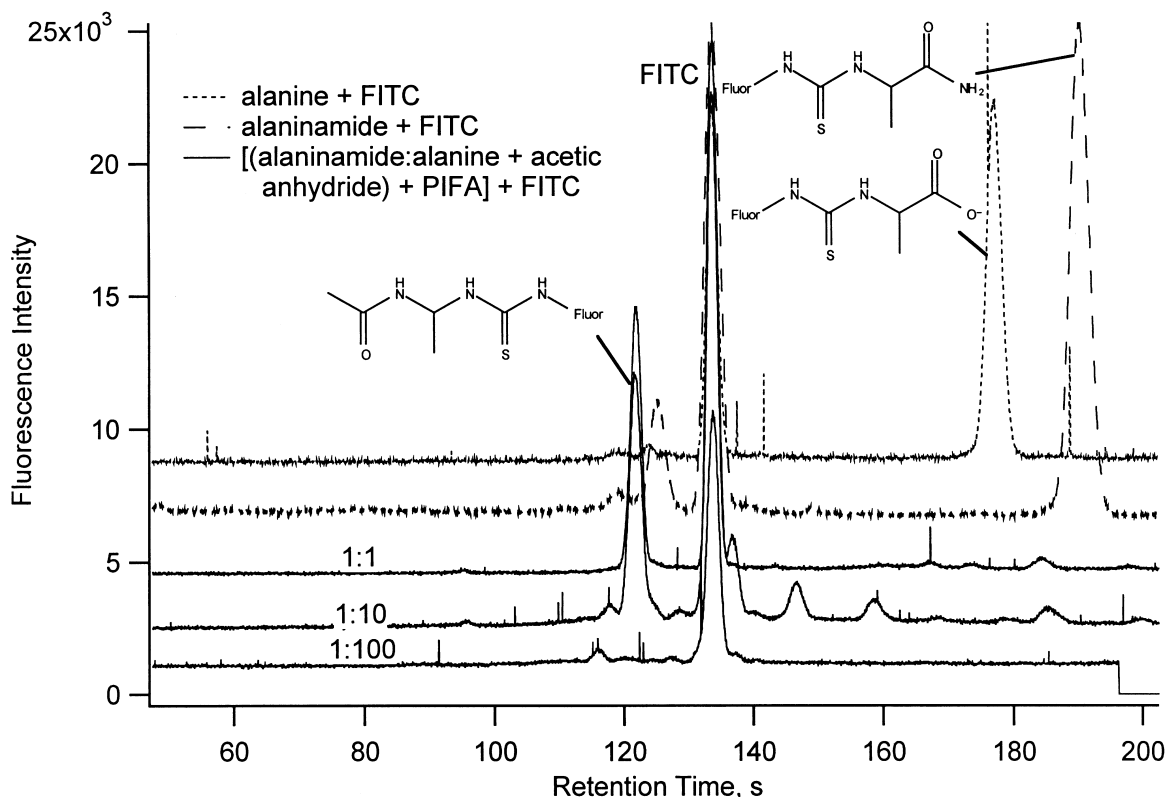


Fig. 6. Acetylation protection of amine groups prior to derivatization of amides. Top two traces: FITC-derivatized alanine (short dash) and alaninamide (long dash); bottom three traces: reaction mixture of alaninamide and alanine, at the concentration ratios given, subjected to full derivatization scheme (Fig. 1) and diluted before injection. Beginning concentration of amine or amide was 33 mM for all traces, except alaninamide was reduced according to the concentration ratio indicated (i.e., 1:10 represents 33 mM alanine + 3.3 mM alaninamide in the initial acetylation reaction mixture). Electrophoresis conditions as in Fig. 5 (50 mM SDS).

than that shown in Fig. 3. To what degree the reactions are reproducible is also unknown.

#### 4. Conclusions

The selective derivatization of amino acid amides in the presence of excess amino acids has been demonstrated. The reactions were easily carried out off-line in reasonable time frames and with reasonable recovery. Eleven of the resulting derivatives have been separated in MECC mode capillary electrophoresis. Elution order was based primarily on hydrophobicity of the side-chain from the original amino acid amide (i.e., partitioning into the micellar phase), and relative hydrophobicity values from

amino acids were reasonable predictors of chromatographic behavior. Separation of less hydrophobic compounds was marginal due to lack of sufficient partitioning. Efficiency of the separation was excellent (generally  $>5 \cdot 10^5$  plates/m), but was limited by Joule heating at high micelle concentrations.

This method appears to be a reasonable means of achieving both high sensitivity and fast analysis time for amide-specific screening. However, all of the reactions were carried out at concentrations that are considerably above the levels expected in biological tissue extracts or serum ( $\mu\text{M}$  or below). In general, experience has shown that FITC reactions do not yield adequate product below  $\mu\text{M}$  levels, and then only with FITC in large excess. Similar limitations may exist for the PIFA reaction; work is in progress

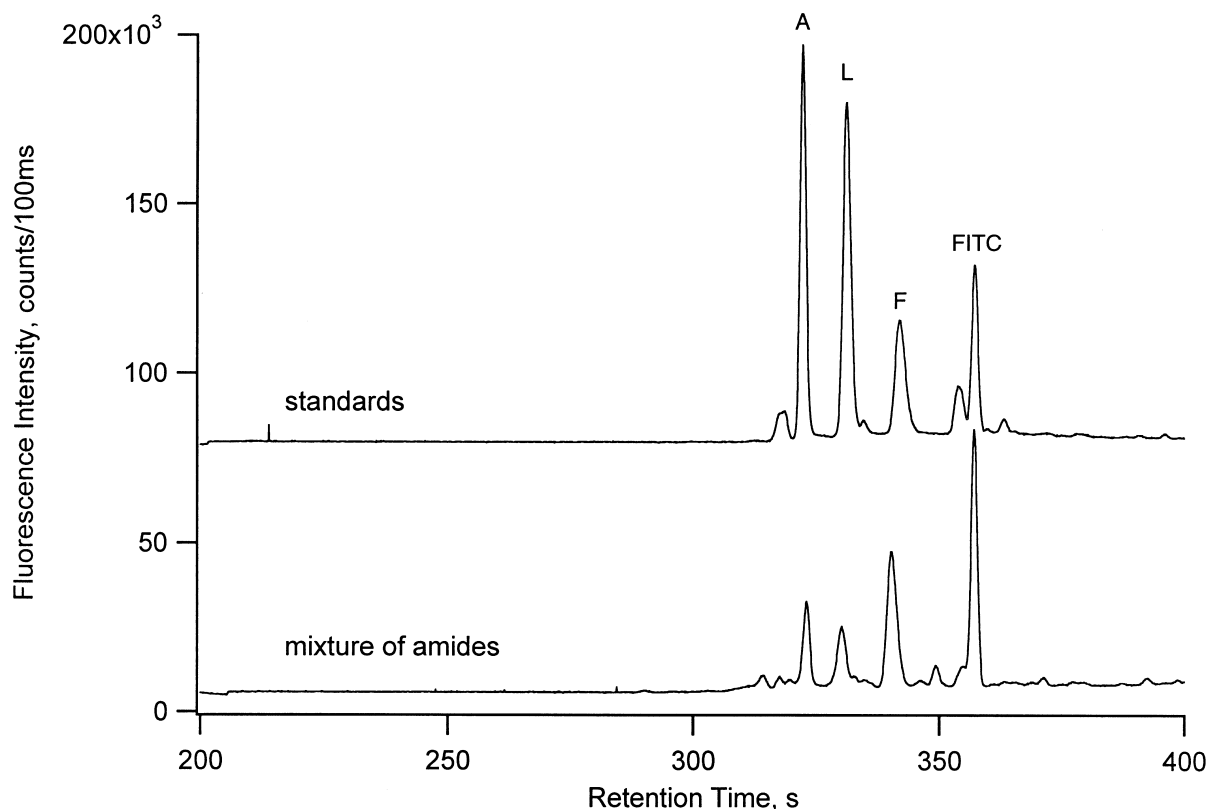


Fig. 7. Demonstration of selective derivatization scheme. Top trace (standards) is an injection of a mixture of individually derivatized, commercially-supplied *N*-acetylamino acid amides; bottom trace is an injection of dilute reaction mixture of 3 amides subjected to the full derivatization scheme depicted in Fig. 1; see Section 2 for details. Electrophoresis conditions as in Fig. 6. Final injected concentrations 6.3 nM each.

to determine kinetic and solvent limitations. However, based on preliminary kinetic information (Fig. 2),  $\mu\text{M}$  levels are probably tolerable. One advantage to fluorescence spectroscopy is the extreme sensitivity; “clean” solutions of FITC can be determined at the  $10^{-13}$  M level with this equipment (unpublished data). Thus, reaction completion is not required, and some of the kinetic limitations can be circumvented. It is possible that extensive sample cleanup and pre-concentration, perhaps online, will be required for practical implementation of this methodology. Labels with better photophysical and chemical properties are also available, though none behave well below 10 nM.

Future work will concentrate on obtaining quantitative data on product recovery and reproducibility as well as spectroscopic data (e.g., fluorescence

quantum yield) on pure product. Several unknown reaction by-products must be identified in order to better understand the reaction and to enable better selectivity in both derivatization and sample cleanup. The use of FITC, mandated in this initial work by ease of use, was clearly the limiting factor in ultimate sensitivity, and will be replaced with other reagents.

#### Acknowledgements

This work was supported by the Samuel and Emma Winters Foundation and the Noble J. Dick Foundation/Duquesne University Faculty Development Fund.

## References

- [1] D.J. Merkler, *Enzyme Micro. Technol.* 16 (1994) 450.
- [2] B.A. Eipper, D.A. Stoffers, R.E. Mains, *Ann. Rev. Neurosci.* 15 (1992) 57.
- [3] J.F. Rehfeld, L. Bardram, S. Blanke, J.R. Bundgaard, L. Friis-Hansen, L. Hilsted, A.H. Johnsen, M. Kofod, H.R. Lüttichau, H.-J. Monstein, C. Nielsen, F.C. Nielsen, L.I. Paloheimo, K. Pedersen, J. Pildal, J. Ramlau, W.W. van Solinge, U. Thorup, L. Odum, *Tumor Biol.* 14 (1993) 174.
- [4] W.D. Odell, A.R. Wolfson, *Am. J. Med.* 68 (1980) 317.
- [5] M.L. Kochman, J. DelValle, C.J. Dickinson, C.R. Boland, *Biochem. Biophys. Res. Commun.* 189 (1992) 1165.
- [6] N. Hoosein, P.A. Kiener, R.C. Curry, M.G. Brattain, *Exp. Cell Res.* 186 (1990) 15.
- [7] L. Saldise, A. Martínez, L.M. Montuenga, A. Treston, D.R. Springall, J.M. Polak, J. Vázquez, *J. Histochem. Cytochem.* 44 (1996) 3.
- [8] K.E. Schwartz, A.R. Wolfson, B. Forster, W.D. Odell, *J. Clin. Endocrinol. Met.* 49 (1979) 438.
- [9] K. Yamaguchi, K. Abe, N. Yanaihara, *Biomed. Res.* 13 (1992) 279.
- [10] D. Robinson, M. Tieder, N. Halperin, D. Burshtein, Z. Nevo, *Cancer* 74 (1994) 949.
- [11] T. Tsukamoto, M. Noguchi, H. Kayama, T. Watanabe, T. Asoh, T. Yamamoto, *Int. Med.* 34 (1995) 229.
- [12] G.S. Wand, C. May, V. May, P.J. Whitehouse, S.I. Rapoport, B.A. Eipper, *Neurology* 37 (1987) 1057.
- [13] K. Tatamoto, V. Mutt, *Proc. Natl. Acad. Sci. USA* 75 (1978) 4115.
- [14] H.P.J. Bennett, S. Solomon, *J. Chromatogr.* 359 (1986) 221.
- [15] W.H. Simmons, G. Meisenberg, *J. Chromatogr.* 266 (1983) 483.
- [16] J.C. Hill, G.M. Flannery, B.A. Fraser, *Neuropeptides* 25 (1993) 255.
- [17] M. Albin, P.D. Grossman, S.E. Moring, *Anal. Chem.* 65 (1993) 489A.
- [18] T. Bergman, B. Agerberth, H. Jörnvall, *FEBS Lett.* 283 (1991) 100.
- [19] A.J. Gee, L.M. Groen, M.E. Johnson, *J. Chromatogr. A*, submitted for publication.
- [20] D.L. Gallaher Jr., M.E. Johnson, *Appl. Spectrosc.* 52 (1998) 292.
- [21] M.R. Almond, J.B. Stimmel, E.A. Thompson, G.M. Loudon, *Org. Synth.* 66 (1988) 132.
- [22] R.H. Boutin, G.M. Loudon, *J. Org. Chem.* 49 (1984) 4277.
- [23] G.M. Loudon, A.S. Radhakrishna, M.R. Almond, J.K. Blodgen, R.H. Boutin, *J. Org. Chem.* 49 (1984) 4272.
- [24] C. Saby, K.B. Male, J.H.T. Luong, *Anal. Chem.* 69 (1997) 4324.
- [25] N. Matsubara, S. Terabe, in: P.G. Righetti (Ed.), *Micellar Electrokinetic Chromatography in the Analysis of Amino Acids and Peptides*, CRC Press, Boca Raton, FL, 1996, p. 155.
- [26] T.E. Creighton, *Proteins. Structures and Molecular Properties*, W.H. Freeman, New York, 2nd ed., 1993, p. 154.
- [27] Y. Zhang, E. Arriaga, P. Diedrich, O. Hindsgaul, N.J. Dovichi, *J. Chromatogr. A* 716 (1995) 221.
- [28] M. Albin, R. Weinberger, E. Sapp, S. Moring, *Anal. Chem.* 63 (1991) 417.
- [29] S. Terabe, K. Otsuka, T. Ando, *Anal. Chem.* 57 (1985) 834.
- [30] J. Bergquist, S.D. Gilman, A.G. Ewing, R. Ekman, *Anal. Chem.* 66 (1994) 3512.